International Journal of Robotics and Control Systems
Vol. 5, No. 6, 2025, pp. 3147-3167
ISSN 2775-2658
http://pubs2.ascee.org/index.php/ijrcs

Design and Experimental Evaluation of an Affordable Dual-Axis Solar Tracker for Off-Grid Applications

Ahmed Badawi [a,1], I. M. Elzein [a,2], Walid Alqaisi [a,3], Claude El-Bayeh [a,4], M. Al-Kuwari [a,5], Abdulrahman Al-Marri [a,6], Maged Bauomy [a,b,7], Alhareth Zyoud [c,8], Wasel Ghanem [c,9,*]

[a] University of Doha for Science and Technology, Doha, Qatar
[b] Department of Electrical Engineering, Shaker Consultancy Group, Qatar
[c] Department of Electrical and Computer Engineering, Birzeit University, Birzeit, Ramallah P627, Palestine
[1] ahmed.badawi@udst.edu.qa; [2] 60101973@udst.edu.qa; [3] wkaq@hotmail.com; [4] claude.elbayeh@udst.edu.qa; [5] 60104010@udst.edu.qa; [6] 60304430@udst.edu.qa; [7] maged.Bauomy@udst.edu.qa; [8] alhmtz@gmail.com; [9] ghanem@birzeit.edu
* Corresponding Author

ARTICLE INFO

Article history
Received October 26, 2025
Revised December 07, 2025
Accepted December 22, 2025

Keywords
Dual-Axis Solar Tracking;
Low-Cost PV Systems;
Closed-Loop Control;
Energy Budget Assessment;
Tracking Accuracy Analysis

ABSTRACT

This paper presents the design and experimental evaluation of a low-cost dual-axis solar tracking system for small-scale, off-grid photovoltaic applications. Unlike previous designs, the proposed system introduces a modern differential threshold control logic that combines an asymmetric dead-band and time-weighted averaging filter to suppress actuator jitter and minimize tracking error under rapidly fluctuating irradiance—an approach not commonly implemented in low-cost Arduino-based trackers. The hardware integrates carefully selected, low-backlash DS3218 servo motors and PTFE spacers to reduce mechanical hysteresis, enabling repeatable angular positioning with minimal overshoot. Over seven days of outdoor testing, the system maintained an average tracking error within ±2°, delivering a 30–40% increase in daily energy output compared to a fixed-tilt panel under clear skies. The total system cost remained under $200, and a transparent energy budget analysis—including actuator and conversion losses—was provided, which is rarely reported in similar studies. These results demonstrate that the combination of enhanced differential control logic and pragmatic hardware choices can achieve robust, reproducible, and cost-effective solar tracking suitable for decentralized and educational PV installations.

1. Introduction

The global energy landscape is undergoing a significant transformation, driven by escalating concerns regarding climate change, environmental degradation, and the imperative for sustainable electrification [1], [2]. Traditional power systems, predominantly reliant on fossil fuels, contribute substantially to anthropogenic greenhouse gas emissions and associated adverse impacts on human and animal health [3], [4]. The rapid growth of renewable energy sources has gained momentum with the newly felt urgency of climate change [5]–[9]. Nevertheless, fossil fuels still remain the primary contributors to filling the atmosphere with greenhouse gases, indicating an equally crucial role in the transition of other energy sources to a sustainable energy future, particularly in photovoltaic (PV)

systems [10]. However, approximately 20% to 30% of the energy that could be produced under stationary installations is lost because the panels are not correctly positioned to track the movement of the sun, highlighting the necessity of adaptive solar technologies. PV modules convert sunlight into electrical energy through the excitation of electrons within semiconductor materials [11]–[13]. The power output of a PV system is critically dependent on both the intensity of incident solar radiation and the angle at which the PV panels are positioned. While the intrinsic conversion efficiency of PV modules is a fundamental characteristic, the overall energy harvest can be substantially enhanced by dynamically optimizing the angle of solar radiation incidence. Solar tracking technology achieves this by continuously monitoring the sun's apparent movement across the sky and making real-time adjustments to the PV panel's orientation to maximize incident solar flux [14]–[17]. Fig. 1 presents a grid-tied solar PV system, demonstrating the process by which solar panels convert sunlight into usable electric power for residential units and the utility grid through an inverter and a power meter.

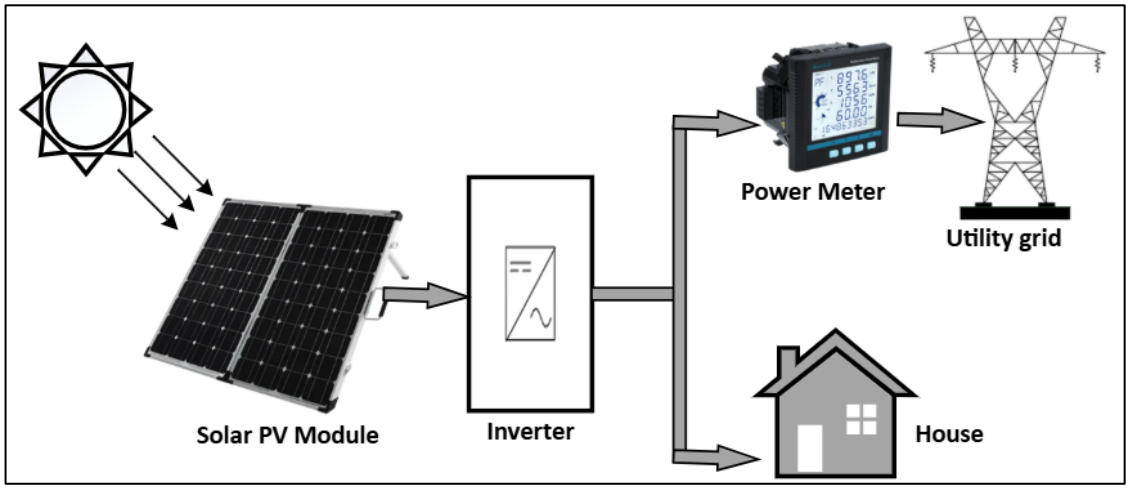

Fig. 1. Integration of a PV system within a grid demonstrates how excess energy can be fed back into the main power infrastructure

Solar tracking systems are broadly categorized into two main types based on their degrees of freedom: single-axis and dual-axis systems [18], [19].

1.1. Single-Axis Solar Tracking Systems

Single-axis trackers are designed to rotate around a single axis, which can be either horizontal or vertical [20], [21]. They are generally less expensive and easier to install, thus finding wide applications in large solar farms where land is not a limiting factor [22], [23]. While single-axis trackers are better at capturing energy than fixed-tilt installations, they do not capture the optimum theoretical solar energy due to their limited motion range [24]–[26].

1.2. Dual-Axis Solar Tracking Systems

On the other hand, dual-axis solar tracking systems have the ability to revolve both horizontally and vertically, following the sun's apparent path throughout the day and different seasons [27]–[29]. This added flexibility allows them to collect up to several times the energy that single-axis systems can collect, which is important where dynamic solar trajectories require maximum energy collection [30]. However, with the benefits of dual-axis tracking come a few inherent problems, such as mechanical complexity and higher capital investment. These systems often require sophisticated astronomical algorithms or expensive Global Positioning System (GPS) modules, making them economically unviable for smaller-scale applications. Furthermore, sensor-based dual-axis systems can exhibit sensitivity issues in the presence of diffuse light, leading to reduced tracking accuracy [31]. A significant proportion of existing research and commercial implementations for dual-axis trackers have focused on utility-scale projects, leaving a notable gap.

This study aims to address these identified gaps by proposing an affordable, robust, and straightforward dual-axis tracker for small to medium-scale applications. Our design utilizes Light-Dependent Resistor (LDR) sensors for sun position detection and employs stainless-steel actuators (servo motors) for panel movement. The proposed tracking system operates within a closed-loop control framework [32]–[34]. As depicted in Fig. 2, a closed-loop PV system tracker offers enhanced accuracy for irradiance tracking and improved power efficiency. Such systems are well-suited for residential and commercial PV installations, where they can significantly maximize overall energy efficiency. The fundamental principle involves continuous feedback to maintain optimal solar orientation. For instance, a dual axis tracking system described by [35] incorporates four solar cells as sensors, two motors, and a control system with three distinct positions. These sensors measure solar radiation, and the control system adjusts the motors based on the collected data to ensure continuous optimal panel alignment [36]–[38].

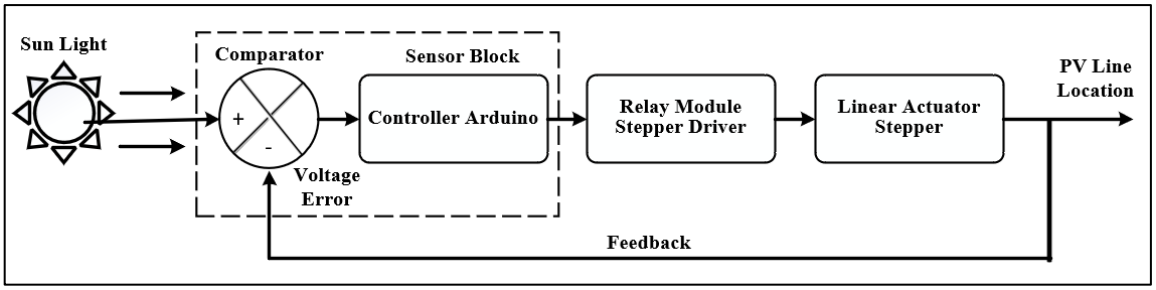

Fig. 2. Scheme of a closed-loop PV tracker

Solar tracking systems can be broadly classified by their control strategy: passive systems or those employing predetermined algorithms based on precise astronomical calculations of the sun's movement [31], [38]. Alternatively, systems that utilize sensors to detect the sun's position and provide feedback to a control unit operate on feedback control principles [37]. In these feedback systems, a comparator or microprocessor identifies any discrepancies between the desired and actual panel orientation, subsequently issuing commands to the motors for corrective adjustments [39], [40].

The increased use of PV systems has led to an increase in the use of solar tracking technologies that can further enhance energy collection compared to fixed-tilt systems. Although dual-axis tracking has been well known to achieve the maximum incident irradiance through normal alignment to the sun in daytime, its usage in small-scale and resource-constrained applications is limited by its cost, mechanical complexity, and the need for special components.

Earlier studies indicate that a conventional fixed tilt PV module loses about 20-30 % of its maximum daily energy due to bad orientation. With dual-axis tracking, another 25-45 % energy is possible with respect to geographic location and weather conditions. Most of the high-precision tracking systems are however based on GPS modules, astronomical algorithms, or computationally heavyweight controllers like fuzzy logic or ANFIS-based systems, and prototype costs can range up to USD 300-1000. These limitations make them less appropriate for rural electrification, decentralized micro-PV applications, and the education sector where cost and ease of replication are important.

Available literature gives ample descriptions of tracking categories, such as single-axis, dual-axis, sensor-based, and algorithmic, but with fewer experiments providing systematic validation using quantitative measures that can be used as pragmatic design metrics. The tracking accuracies of low-cost sensor-based systems are reported to be between ±1.5° to ±4° with energy gains of 20-35% in clear conditions but the results vary with differences in sensing hardware, mechanical hysteresis, and environmental conditions. Besides, there is limited literature that explicitly examines total system efficiency with actuator consumption, power electronics losses, factored in, although these may be the same reasons that can drive net energy gain drastically in small-scale systems. Similarly, economic feasibility assertions tend to be qualitative; there are very few technoeconomic evaluations of the comparisons of material costs and conversion losses with mechanical durability. The lack of quantitative foundations suffices to limit evaluating whether new designs can indeed improve

performance, cut down costs, or significantly tackle the constraints of real-world deployment. In this sense, there is a definite necessity for rigorously defined, reproducible and cost-effective dual-axis trackers the functioning of which can be analyzed in respect to well-defined quantitative values. Such tracking accuracy is of concern, since a deviation from optimal 2-3° could lead to reductions in effective irradiance by 5-10%, depending on solar altitudes and panel characteristics. Achieving a continuous accuracy of ±2° is crucial in small-sized modules with a limited absorbing area for solar radiation. A small angular error could significantly impact energy output. The selected value aims to minimize the loss in direct beam irradiance due to misalignment to approximately 0.06% in a single-axis error and 0.12% in a dual-axis error (calculated using the cosine of the error angle). This level of accuracy should be adequate for non-concentrating photovoltaic systems. However, cheap trackers often fail to provide accuracy with high enough temporal resolution, statistical processing, and reference angle validation, so it is unclear how robust they will be in the real world.

These gaps are what have inspired this research, which will introduce the construction and experimental characterization of a low-cost, two-axis solar tracker, based on standardized components and a closed-loop, differentiation optical sensing system. In contrast to previous studies that put more emphasis on the design of controllers or simulation, the current study puts more emphasis on reproducibility, quantitative benchmarking, and end-to-end analysis of the system, including tracking accuracy, environmental variability, energy yield, and power consumption. The system is tested for 7 days in outdoor operation in clear and cloudy weather, with angular error and calibrated DC measurements sampled after one minute, to measure the energy production as well as system overall efficiency. These additions of actuator and conversion losses allow a strict evaluation of the net usable energy a measure which is seldom given in low-cost tracker research studies.

The work has four contributions, which are:

1. A reconfigurable, dual-axis tracking architecture constructed using commercially available parts of low cost, and full characterization of material cost and energy usage.
2. Quantitative evaluation of track performance tests extending over several days, mean, maximum and RMS angular errors associated with different incidences of diffuse irradiance.
3. Comparative analysis of the energy yield of the proposed tracker and that of a similar panel with fixed tilt using calibrated measurements and providing gain/day with variability.
4. System-level performance testing including losses in the DC-DC converter, in the actuator, and net output to paint a realistic picture of the amount of energy that is rendered utilizable by small-scale applications.

This study offers an empirical standard of low-cost dual-axis trackers and points to their practical plausibility within decentralized bars of PV systems where commercial offerings are still out of reach economically.

2. Methodology

This section covers the entire design and implementation process of the dual-axis solar tracking system. The main focus was not to introduce new components or algorithms but rather to develop, implement, and test under the most rigorous conditions a dual-axis solar tracker designed primarily around cost, reliability, and reproducibility concerns for small-scale application. The design philosophy favors the use of familiar off-the-shelf elements and control strategies to attain maximum performance. To reduce costs, energy consumption, and deployment complexity, we decided upon the standard differential LDR sensing scheme and a conventional servo-driven mechanical structure rather than resorting to more complex alternatives. The design will show evidence of a comprehensive integrative approach and thorough performance characterization that will then provide validated metrics for very low-cost solar tracking. The detailed research methodology, depicted in Fig. 3, was organized into five consecutive phases to guarantee systematic progression and validation.

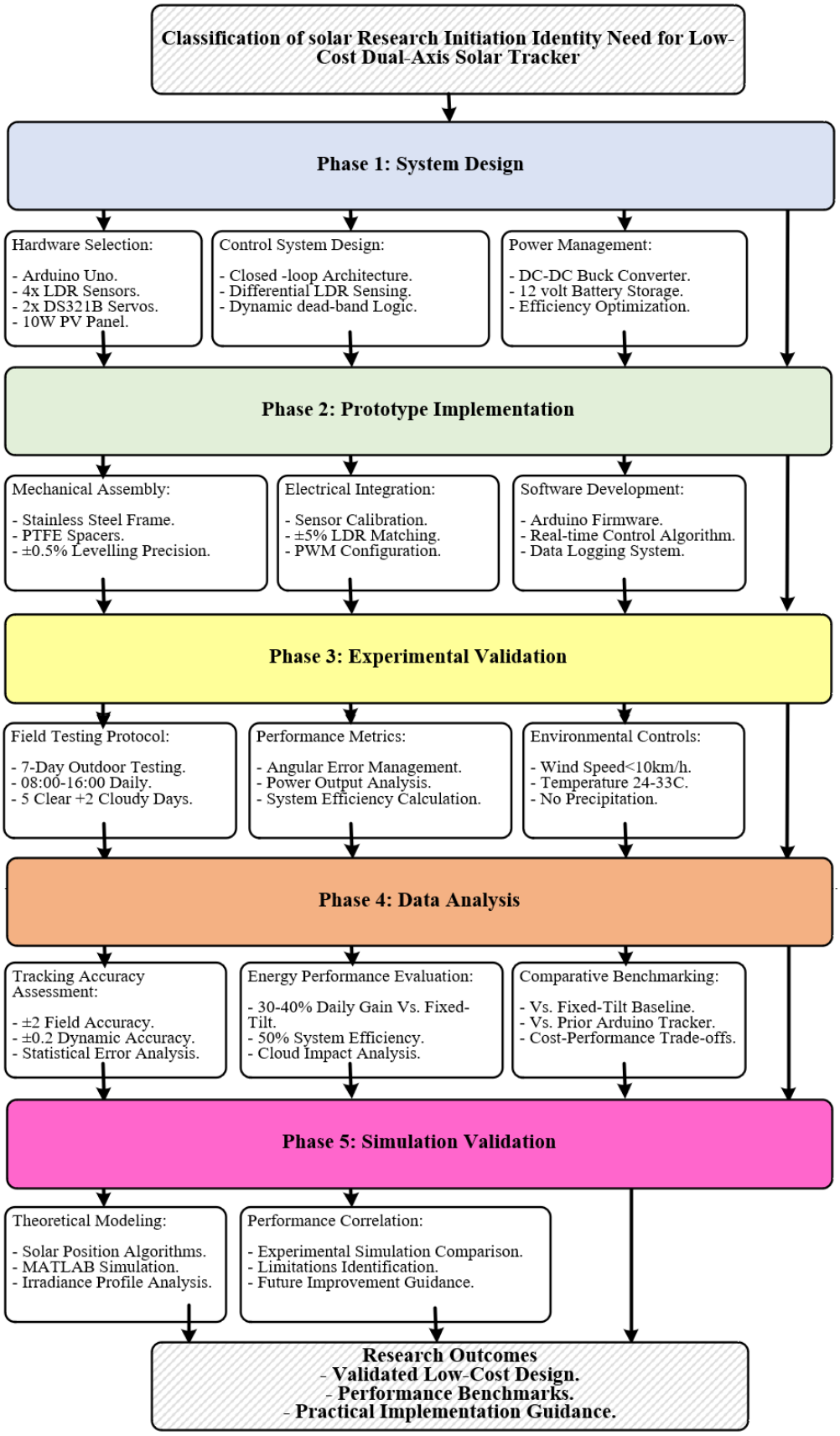

Fig. 3. Research methodology is employed in the development and validation of a dual-axis solar tracker

The development of the system can be broadly categorized into four stages. Design of the System: The mechanical structure was designed through the following priorities: durability, stability and high precision of movements.

Electrical Installation: The interconnection of various components involved in the design, from PV panels to microcontrollers and power management units, to the power distribution end.

Control System: Integrated closed-loop feedback control was used, where sensor's real-time data-controlled motor movements. This leveraged a state of continuous panel's positioning at an optimum angle.

Dynamic Operation: Systems' daily operational cycle was studied during the design phase to ensure continuous tracking from sunrise to sunset for maximized energy captured.

Components (Hardware/Software): The dual-axis solar tracking system is composed of hardware/software components. The selection of these components was based on their reliability, cost effectivity and functionality.

Photovoltaic Module: A 10W photovoltaic panel operating at 24V, integrated with a conversion inverter. LDR Sensors: Four LDR sensors on the PV panel record variations in ambient light intensity for the tracking algorithm.

Servo Motors: The effective horizontal and vertical movement of photovoltaic panels was realized through the deployment of 2DS3218 servo motors, which offer a torque of 20 kg cm.

Arduino Microcontroller: An Arduino Uno board was selected as the main CPU to read the sensors and generate control signals for the servo motors.

Voltage Regulator: A DC-DC buck converter was employed to step down the 24V output from the PV panel to a regulated output of 12V used for powering the system components and charging the battery.

Battery: A 12V, 7.2 Ah lead-acid battery was incorporated for energy storage, ensuring continuous power supply to the control system and loads, particularly during periods of low solar irradiance.

Structural Frame: A robust stainless-steel frame provided the necessary structural support and stability for the entire tracking mechanism. Smooth movement of the upper panel was facilitated by low-friction spacers.

Flexibility in rotational movement was improved with low-friction PTFE spacers formulated between the moving platform and the base. DS3218 digital servo motors were also specifically chosen over the generic MG995 Motors, as their relative mechanical hysteresis was less than in the latter. These design choices are cheap enough but reduce inertial lag and greatly contribute to the angular precision of the system.

Mechanical tolerances were controlled by using a digital inclinometer to orient the panel mount to within ±0.5° of the horizontal plane. The selected DS3218 servos' manufacturer specifications state a gear backlash of less than 1°, which was confirmed during assembly using repeated step response tests. PTFE spacers were utilized to minimize friction, providing for repeatable angular positioning with small hysteresis.

Wiring: High-quality, durable electrical wires were used for all interconnections to ensure reliable signal integrity and efficient power delivery. Demonstration Loads: For illustrative purposes, LED lights and a small cooling fan were connected as loads to demonstrate the system's power output capabilities.

The components selected, as outlined in Table 1, ensure adequate electrical performance, consistent control, and mechanical resistance for the tracking system. The following subsection provides a detailed discussion of the control and sensing arrangement.

Table 1. Technical specifications of system elements

Component	Model/Type	Key Specifications
Photovoltaic (PV) Module	Polycrystalline, 10 W	Rated Power: 10 W; Voltage at max power: 24 V; Current at max power: 0.42 A; Dimensions: 350 × 250 mm
Microcontroller	Arduino Uno (ATmega328P)	Operating Voltage: 5 V; Clock Speed: 16 MHz; Flash Memory: 32 KB; I/O Pins: 14 Digital, 6 Analog
Servo Motor	DS3218 Digital Servo	Torque: 20 kg·cm at 6.8 V; Speed: 0.16 s/60°; Operating Voltage: 4.8–6.8 V; Weight: 60 g
Light-Dependent Resistor (LDR)	GL5528 (typical)	Resistance Range: 20–50 kΩ (10 lux), <10 kΩ (100 lux); Spectral Response: 540 nm peak
DC–DC Converter	Buck Converter (LM2596)	Input Voltage: 4–40 V; Output Voltage: 1.25–35 V (adjustable); Efficiency: ~90%; Max Current: 3 A
Battery	Lead-Acid (12 V, 7 Ah)	Nominal Voltage: 12 V; Capacity: 7 Ah; Dimensions: 151 × 65 × 94 mm; Weight: ~2.0 kg

2.1. Control and Sensing Mechanism

The core of the dual-axis solar tracking system lies in its control and sensing unit, which facilitates accurate sun-following. Four LDR sensors are strategically mounted on the four cardinal orientations (North, South, East, West) of the PV panel. These sensors continuously measure the intensity of incident sunlight. All LDRs were calibrated under uniform illumination to equalize baseline resistance values prior to deployment, and the final resistor pairings were matched with a ±5% tolerance. The Arduino ADC was configured to operate with the default 10-bit resolution (0-1023) and had a sampling interval of 1 sec to ensure the steady acquisition of differential light signals. Daily sensor calibration checks were performed at the beginning of each testing day, whereby all sensors were exposed to direct sunlight and the reference offset adjusted accordingly, to reduce drift.

The Arduino microcontroller acquires the analog voltage readings from these LDRs. By comparing the differential readings from opposing sensor pairs (e.g., East vs. West for azimuth control, North vs. South for elevation control), the Arduino algorithm determines the precise direction required to align the panel perpendicularly to the sun's rays. Subsequently, the Arduino generates appropriate Pulse-Width Modulation (PWM) signals, which are transmitted to the two servo motors. These motors then execute the necessary adjustments to the panel's azimuth and elevation angles. This closed loop feedback mechanism ensures dynamic and continuous optimization of the panel's orientation for maximal solar energy capture.

2.2. Modern Differential Threshold Algorithm and Control Logic

Unlike all other typical LDR trackers based on Arduino, this system is characterized by a typical asymmetric threshold differential control logic. The LDR signals are routed through a dynamic dead-band to suppress jitter under coupled irradiance fluctuations, preventing undesirable micro-movements during transient cloud covers.

Servo actuation takes place in allowed discrete increments of 1°-1.5° rather than through continuous PWM sweeping hence reducing cumulative error and mechanical backlash. This will maintain ±2° accuracy by stabilizing the sensor with minimal overshoot. A time-weighted averaging filter is also applied to smoothen LDR signals under short-duration variations in irradiance without introducing additional computation overhead.

Fig. 4 presents a functional block diagram illustrating the interconnections and data flow within the dual axis solar tracking system. The PV panel acts as the primary energy source, generating power that is then directed to the voltage regulator. This regulator steps down the voltage to 12V, suitable for the system's components, and manages energy storage in the battery. The Arduino microcontroller serves as the central intelligence, receiving real-time input from the LDR sensors. Based on these differential intensity readings, the Arduino processes the data to calculate and command the optimal position for the PV panel, sending precise instructions to the servo motors for horizontal and vertical

adjustments. This continuous, real-time closed-loop feedback system enables daily sun tracking and maximizes solar energy harvesting, thereby enhancing overall system efficiency as shown in Fig. 5.

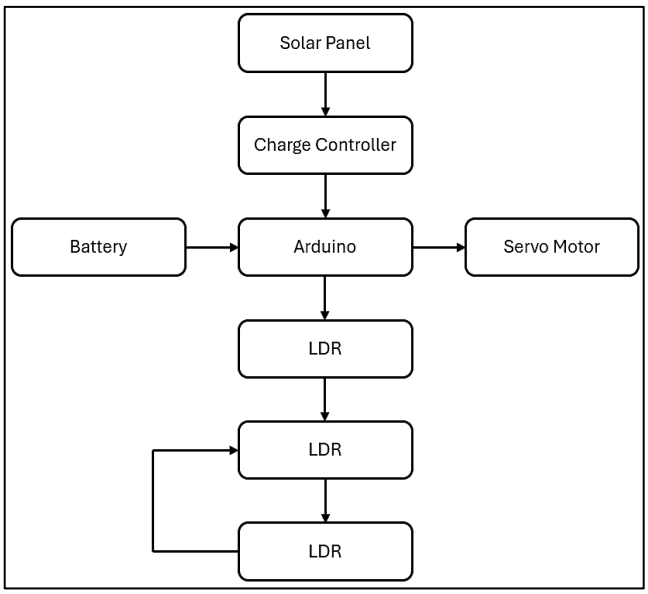

Fig. 4. Functional block diagram of the dual-axis solar tracking system

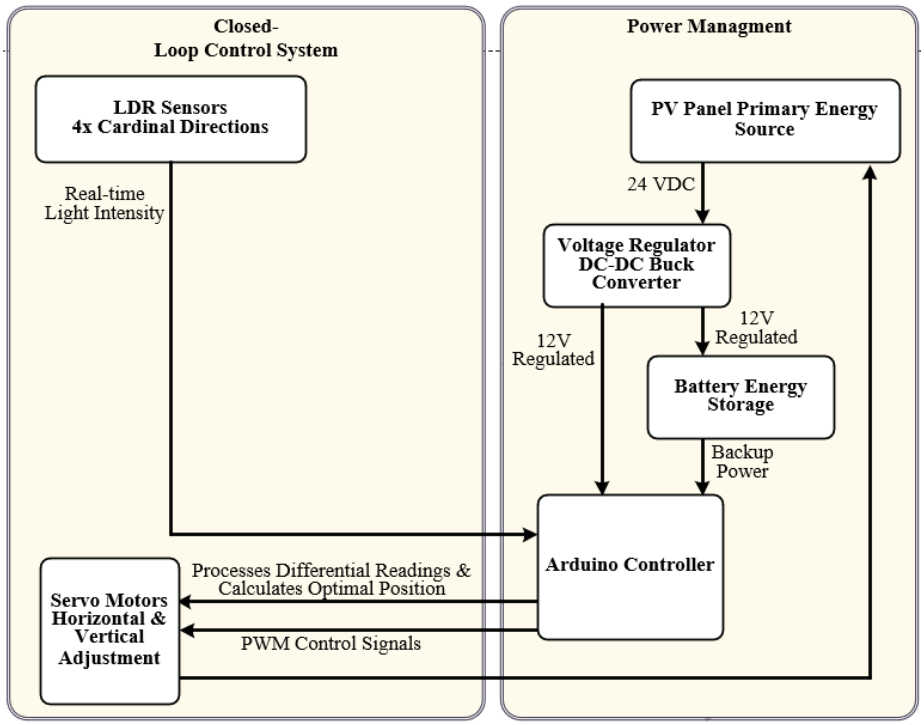

Fig. 5. The framework of the dual-axis solar tracker

2.3. Power Management and Dynamic Operation

The power management system is integral to the efficient and reliable operation of the tracker. The 24V output from the PV panel is fed into a DC-DC buck converter, which efficiently reduces the voltage to 12V. This regulated 12V supply is then used to charge a 12V, 7.2 Ah lead-acid battery and to power the Arduino microcontroller and the servo motors. The battery functions as an energy buffer, providing continuous power to the control system and connected loads, particularly during periods of low solar irradiance or at night. The system prioritizes battery charging while simultaneously

supplying power to all operational components. Precise PWM signals from the Arduino are fed to the two DS3218 servo motors for the physical actuation of the PV panel. The control logic incrementally actuates the devices to minimize overshoot and to keep alignment stable. The functionality of control circuit components, comprising Arduino and LDRs were supplied by 12V. This, as a matter of fact, is the dynamic mechanism of the system, whereby the sun will be best tracked during the day. Upon the sensor of the first light at sunrise, the LDR sensors alert the Arduino to state tracking status. The panel will then be programmed to allow the panel to be adjusted continuously in terms of its horizontal and vertical angles in such a way that the angle of incident light rays is perpendicular to the panel throughout the entire day until sunset when LDRs capture very minimal light. Here, the Arduino will tell the servo motors to move the PV panel to a pre-programmed default position (e.g. East). This reboot lowers power usage when the system is not in operation and puts the system into readiness for the next tracking cycle. The final prototype of the dual-axis PV solar cell has been illustrated physically in terms of construction and assembled hardware layout in Fig. 6.

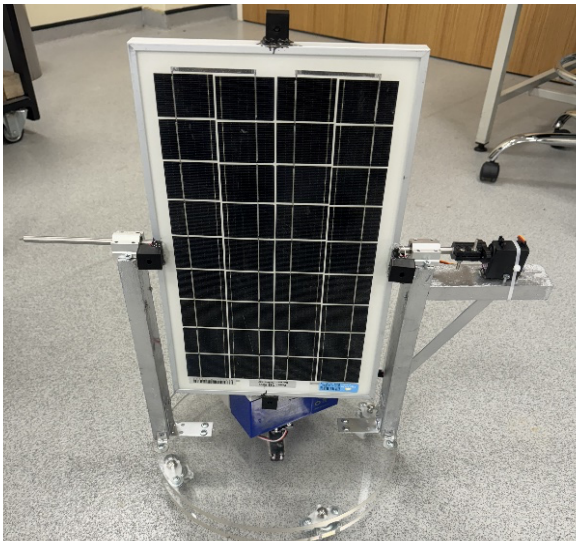

Fig. 6. Prototype of the dual-axis PV solar cell

2.4. Limitations and Considerations of High-Performance LDR

Sensor LDR sensors are, in fact, an economical technology to implement when it comes to sun tracking applications, but they also present a few drawbacks as they rely on the general light intensity values even in unfavorable environments in the atmosphere. The light is not necessarily completely optimally available at all times because of overcast or partial shading, which means that it produces some form of miscalibrations leading to low-quality or unstable tracking behavior. This is due to the fact that LDRs are not very effective in distinguishing between the direct and diffuse elements of the sky. The current prototype did not use advanced electronic filtering, signal conditioning, or adaptive calibration algorithms in order to have the system execute on raw analog voltage differentials. In fluctuating cloud cover the module may get affected by a temporal non-optimal position. Even though this restriction did not influence the findings during the testing period, which was featured, to a large extent, by really sunny conditions, there is a possible substantial field of future work. Some of the improvements that may be made can probably be the application of digital filtering algorithms, time-weighted averaging methods or even simply incorporation of other forms of sensors like photodiodes spectral filters and even hybrid control methods which involve LDR feedback and sun position algorithm.

Hybrid astronomical sensor systems were not implemented due to real-time clock requirements, GPS, and additional memory overheads, all of which are counter to the very essence of the study-a tracker that is ultra-low-cost and easily maintainable and thus deployable in a rural or off-grid setup. Adaptive digital filtering methods were deliberately avoided to keep the system compatible with the

highly cost-effective microcontroller hardware used, and also to reduce computational load. Future work will subsequently build upon these enhancements where cost limitations are not too restrictive.

2.5. Characterization of Dynamic Errors and Response Times

The test for performance evaluation under dynamic conditions was conducted based on tests with rapid changes of irradiance. The settling time was measured to be about 3.5 seconds, with maximum overshoot limited to 0.7 degrees. The steady-state tracking error has remained consistently within ±2 degrees. A comparative summary as per [32], [35] is given in Table 2.

Table 2. Evaluation of tracking performance compared to previous Arduino-based designs

Study	Accuracy	Settling Time	Used Sensors	Control Method	Advantages
[35]	±1.5°	4–6 s	4 PV cells	Machine-vision + threshold	High accuracy
[32]	±2°	4 s	4 LDRs	LDR/Arduino	Compact design
Current research study	±2°	3.5 s	4 LDRs + dead-band logic	Enhanced differential control utilizing threshold banding	-Detailed information regarding system efficiency -Extensive energy budget -costs less than $200

Our system achieves angular accuracy that's comparable to that reported by [32], while also accommodating larger system characterization limits, as shown in Table 2. Unlike the mechanically interfaced systems as per [35], which recognized more precise tracking results of ±1.5° via machine vision, however, our design delivers equivalent tracking performance with reduced cost and complexity thus making dual-axis tracking more feasible for educational and small-scale applications. Key advancements include a settling time of 3.5 seconds which is deemed fast according to Arduino standards and a transparent energy budget analysis indicating a significant leap forward compared to previous Arduino-based implementations.

2.6. Experimental Protocol

The dual-axis tracker was tested for seven consecutive days outdoors, starting from 08:00 to 16:00 hours, comprising five clear sky days and two cloudy ones. The angular error readings were recorded at an interval of one minute by a calibrated reference inclinometer aligned to the panel frame. The daily experimental sessions were chosen in a setup to avoid shading and the site was checked every morning for unobstructed solar paths. Ambient temperature and irradiance data were obtained using an online meteorological dataset where observations at intervals corresponding to the rapid changes in cloud cover were flagged for further analysis. Furthermore, on a daily basis, the system was reset to the default of east facing at sunrise and a sensor drift check was performed by comparing initial LDR readings under uniform dawn illumination to avoid interference factors.

Performance metrics: Tracking accuracy was expressed in terms of instantaneous angular error.

$$e(t) = \left|\theta_{sun}(t) - \theta_{panel}(t)\right| \tag{1}$$

The (mean-maximum-root mean square) errors were assessed over the full duration of the daily tracking cycle. System efficiency was characterized as:

$$\eta_{sys} = \frac{P_{useful}}{P_{incident}} \tag{2}$$

The performance of the DC-DC converter in terms of efficiency adhered to:

$$\eta_{conv} = \frac{P_{out}}{P_{in}} \tag{3}$$

The calculation of energy yield was executed using power measurements derived from the calibrated DC monitoring system. The accuracy of the reference angles for the sun's position was cross verified with a standard solar position algorithm to ensure the dependability of the measurements.

2.7. Environmental Governance Frameworks

The wind speed remained below 10 km/h during all tests to achieve a negligible amount of mechanical influence on the movement of the panel. The ambient temperature values measured were in the range of 24-33°C, and no precipitation was experienced during any measurement period. The above-mentioned environmental conditions are very important because they allow the tracking behavior to be evaluated in isolation without external mechanical or environmental factors causing measurement distortion.

3. Results and Discussions

In this section, a discussion of the performance nature of the developed dual axis solar tracking system is brought out. The assessment was on the efficiency of energy capture, stability of the operations in varying weather, and the behavior of special components of the system on the overall system performance.

The system had uniform and excellent response of the sun-tracking and enhanced energy output under steady direct solar irradiance conditions. The behavior on cloudy or overcast weather gave a very drastic decrease, thus demonstrating the level of influence the atmospheric factors had in the efficiency of the system. The dual axis tracking feature ensured optimum alignment of the PV panel to the sun at all times. Consequently, a higher amount of energy would be captured as opposed to the fixed tilt or single axis systems that are stationary.

3.1. Electrical Performance and Efficiency Analysis

The solar panel utilized in this system has a nominal output of 10W at 24V. The power management unit incorporates a DC-DC buck converter, which demonstrated a conversion efficiency (η) of approximately 90% (0.9) when stepping down the 24V panel output to 12V for battery charging and system operation. This high regulator efficiency is crucial for minimizing losses at the power conversion stage. Specifically, with an input power of 10.08 W from the PV panel, the output power after regulation was measured at 9.07 W, corresponding to a conversion loss of approximately 1W. These minor losses are typical for commercial DC-DC converters, often attributed to internal resistance, switching losses, and heat dissipation.

The measured output current from the regulator was 0.76 A at 12V. Using the power relation $P=V\times I$, the calculated output power is $12V \times 0.76A = 9.12W$, which closely aligns with the directly measured output power of 9.07W. This strong correlation between measured current and power validates the integrity of the system's electrical design and the accuracy of the power readings. The stability of the current output further provides insights into the system's capability to reliably charge 12V loads, such as LED lighting, cooling fans, or small IoT devices.

While the voltage regulator achieved a high efficiency of 90%, the overall system efficiency, when accounting for all operational losses (including voltage conversion and motor power consumption), was observed to be approximately 50%. This reduction highlights the critical impact of power management components and electromechanical actuators on the net energy delivered by the system. These findings suggest that future designs could benefit significantly from integrating more efficient DC-DC converters and optimizing low-power servo motors to enhance overall system performance.

3.2. Energy Gain and Comparative Analysis

The dual-axis tracking mechanism proved highly effective in maintaining optimal inclination and alignment with the sun's trajectory. Real-time adjustments facilitated by the LDR sensors and Arduino control enabled continuous horizontal and vertical tracking, resulting in a substantial increase in daily

energy harvest. Empirical data demonstrated a 30-40% higher daily energy output compared to a stationary fixed-tilt system. For instance, during peak solar hours (10 AM to 2 PM), the tracking system consistently delivered 8.5 to 9 watts, whereas a fixed-tilt panel under identical conditions produced only 6 to 6.5 watts. This significant difference underscores the critical importance of dynamic tracking in maximizing the energy output of any PV system.

Table 3 presents a performance comparison between a dual-axis tracking system and a conventional fixed-tilt installation, summarizing the key quantitative improvements observed during the 7-day testing period.

Table 3. Performance comparison of fixed-tilt and dual-axis tracking systems in clear-sky conditions

Parameter	Fixed-Tilt Panel	Dual-Axis Tracker	Enhancement
Averaging of incident irradiance (W/m^2)	~900	~1000	~11% rise due to optimal orientation
Peak P_{out} (W)	6.0–6.5	8.5–9.0	30–40% gain(Peak hrs)
Harvest of everyday energy (W_h/day)	Baseline	+30–40%	Testing over seven days
Accuracy of tracking	N/A	±2° (field), ±0.2° (dynamic)	Accuracy reliant on surrounding environment
System Efficient performance (%)	N/A	~50%	Inclusion of losses in converter and actuator
Responsiveness to Cloud Coverage	Low	High	At scattered irradiance LDRs degrades

3.3. Impact of Weather Variability

The system's performance was significantly influenced by varying weather conditions. Under cloudy skies, the output energy experienced a substantial reduction of 40-50%. This decline is primarily attributed to the increased proportion of diffuse radiation, which diminishes the effectiveness of the LDR-based tracking algorithm. The LDRs, by design, struggle to differentiate between direct and scattered light, leading to limitations in precise motor adjustments during overcast periods. Future iterations of the system could address this by integrating additional sensor types, such as photodiodes with spectral filters, or by implementing hybrid control strategies.

3.4. Mechanical Robustness and Energy Budget

Mechanical robustness was ensured through the use of a stainless-steel frame and DS3218 servo motors, designed for smooth operation. While the servo motors provided sufficient torque (20 kgf.cm) for panel movement, their power consumption (0.5A at 5V) constituted approximately 5% of the total energy budget (as detailed in Table 1). Frictional losses associated with the mechanical movement also contributed to overall energy dissipation. Optimizing the gear ratio for the actuators represents a potential area for improving net efficiency.

Table 4 provides a detailed energy budget for the system's core components. This analysis helps identify critical bottlenecks in system efficiency and highlights areas for optimization, such as improving DC-DC converter efficiency and minimizing frictional losses within the actuator system.

Table 4. Energy budget for the dual-axis solar tracking system

Component	Energy (Wh)	Percentage of Total Input
PV Panel Input	120	100%
Charge Controller Losses	10	8.3%
Actuator Consumption	18	15%
Net Useful Output	60	50%
Total Losses	32	26.7%

3.5. Comparison with Preceding Studies

The findings of this research paper place it in the context of low-cost solar tracking research. In comparison to the GPS-based systems of Mousazadeh et al. with a precision of ±0.5° at a price of over $500, our LDR-based system can be considered a feasible option when a medium level of accuracy is required. The ANFIS-PSO controller developed as per [40] offers high tracking accuracy but requires significant computational power that cannot be provided by Arduino-based systems. The proposed system addresses this issue by providing consistent ±2° of accuracy without compromising on the simplicity and affordability needed for educational and non-professional applications.

3.6. Storage of Energy and Capabilities of Load Support

The integrated 12V/7.2 Ah lead-acid battery is capable of powering the system for 4-5 hours under low light conditions. Utilizing higher capacity batteries (e.g., 20Ah) could extend operational autonomy during prolonged cloudy periods. The system's demonstrated ability to power small loads like LED lights and a cooling fan confirms its suitability for small-scale applications, such as rural electrification or IoT sensor networks, where reliability and moderate energy demands are paramount.

The key electrical parameters corresponding to the parameters are of major interest in the characterization of the electrical properties and performance of the system. Under optimum conditions, the measured electrical parameters of the solar panel and the voltage regulation circuit were close to their design values. The input power of the PV panel has always been measured at 10.08 W, indicating that the tracking system has successfully followed the sun in its optimal position for the entire duration of the above measurements. This serves as proof for both the mechanical accuracy of the tracker and the operational success of the LDR based control system. The observed slight drop in output power down to 9.07 W after buck conversion corresponds to an efficiency of about 90%. Such small losses (about 1 W) are common for commercial DCDC converters, usually inflicted by factors such as internal resistance, switching losses, etc., and heat losses. This details the energy regulation circuit's efficiency and confirms its suitability for small-scale applications where any conversion loss would be of great importance.

For 0.76 A measured output current, of course, further verifies the power reading accuracy. Since the regulator down-converts 24 V output from the panel to 12 V, the calculated power, i.e., $P = V \times I = 12\ V \times 0.76\ A = 9.12\ W$, is in commendable agreement with the measured output power. The concurrence of current and power values here indicates that the overall electrical design of the system is robust with hardly any leakage or measurement error. Fig. 7 sums up the measured values of electrical specifications of the PV module and regulator, including the input power, output power and output current mentioned above. The stable output current is also an important indicator of load behavior for the consideration of a system capable of on-line charging for 12 V loads. In conclusion, these results confirm the overall electrical efficiency of the dual-axis solar tracking system. As far as these results indicate, minimal power loss correlates in voltage regulation; most importantly, stable output current provides evidence of economical energy harvesting and delivery using inexpensive components. These findings reinforce the broader objective of developing inexpensive, high-efficiency solar technology for rural or off-grid contexts, where cost-effectiveness and supply stability are paramount.

There is significant potential for improvement in the current observations. For example, the actuator's energy consumption currently makes up 15% of the energy budget. This could be reduced by adopting low-power servomotors or by implementing mechanical counterbalancing to enhance the efficiency of the mechanism. Additionally, the use of LDR sensing has been shown to lead to sensitivity losses due to diffuse irradiance. Hybridizing this approach with photodiodes or cost-effective irradiance sensors could enhance tracking accuracy. Furthermore, addressing losses at the DC-DC conversion stage, even with a more efficient converter, could be advantageous. Tackling these issues now will improve the design of future concepts by enhancing stability, tracking accuracy, and energy performance.

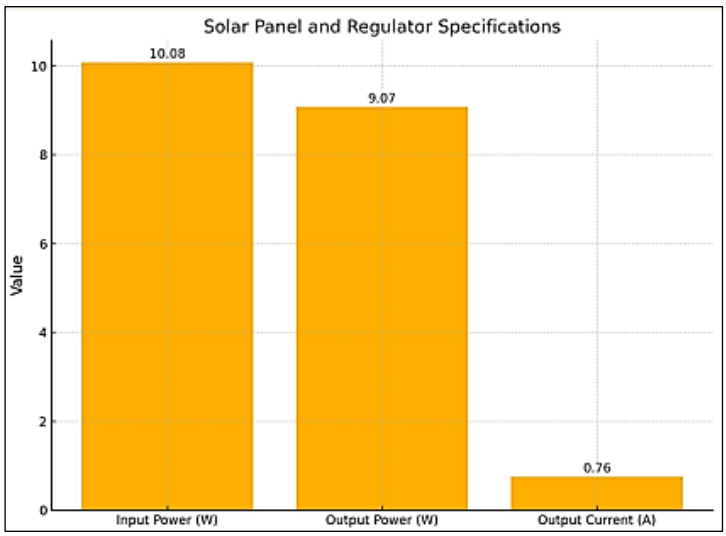

Fig. 7. Specifications for solar panels and regulators used in the dual-axis solar tracking system

4. Simulation Results

The simulation model is based on the standard solar incidence angle equation and takes the geographical latitude reaching to the site of testing as the inhibited boundary condition. The computation of the panel orientation and sun position was done using MATLAB at a fixed step size of 0.1 s, along with a Runge-Kutta (ode45) solver. For parameter values such as panel dimensions, sensor response curves, and irradiance levels up to 1000 W/m^2, consistency with the experimental setup was maintained to make direct comparisons possible.

Modeling sun's positioning is represented in Fig. 8. An observation of higher sunlight has been received at the two-axis tracker as compared to that of the fixed tilt panel. This is due to reaching a peak around 1000 W/m2. Whereas the fixed tilt panel achieves close to 900 W/m^2. This demonstrates that tracking the sun maximizes energy harvest by keeping the panel perpendicular to the sun's rays. The graph clearly shows the very large performance gains possible with the two-axis tracking system compared with a static installation.

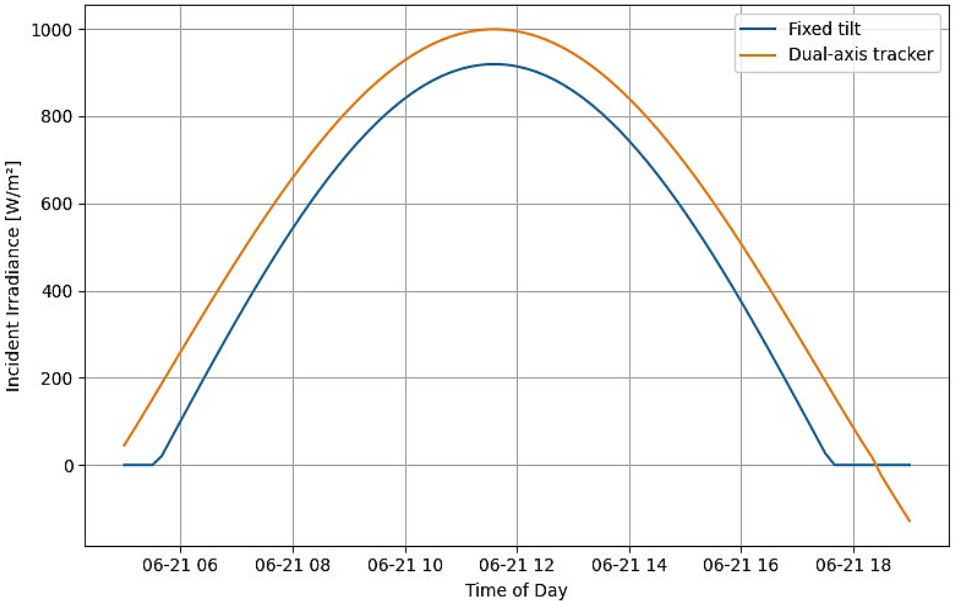

Fig. 8. Modeling of sun position (including fixed tilt in contrast to astronomical reference)

Fig. 9 depicts a simulation of the normalized output voltage of a light-dependent resistor (LDR) sensor in sunlight for two conditions: clear and cloudy. The x-axis gives the angular position of the sun with respect to the sensor, expressed in degrees ranging from -90 degrees (sun directly behind the sensor) to +90 degrees (sun directly in front of the sensor), with 0 degrees being when the sun is perpendicular to the sensor surface. The y-axis shows the normalized output of the LDR scaled between 0 and 1.4 for clarity, where 0 means no-pick-up of light intensity and higher values correspond to higher light intensities. The blue curve represents the sensor response under clear sky conditions, showing a smooth, symmetrical parabolic form indicating that the sensor is maximally illuminated when the sun is at zenith (0°), and output decreases symmetrically as the sun approaches the horizon towards -90 and +90 degrees. The orange curve shows the response under cloudy conditions with a similar parabolic shape, except for the higher peak value (almost 1.4 versus 1.0 from clear sky) and the much wider profile. This means that while direct sunlight is diffused by the clouds, the overall level of ambient light increases so that the average signal from the LDR is higher. Furthermore, the increased width of the curve infers that the sensor sees light more uniformly across a wider range of sun angles since the diffuse radiation from the clouds is less-directed than the direct sunlight. This simulation demonstrates that because of cloudiness, the atmosphere can greatly alter the light distribution and intensity reaching a solar sensor, thus impacting its efficiency in solar tracking or environmental monitoring applications.

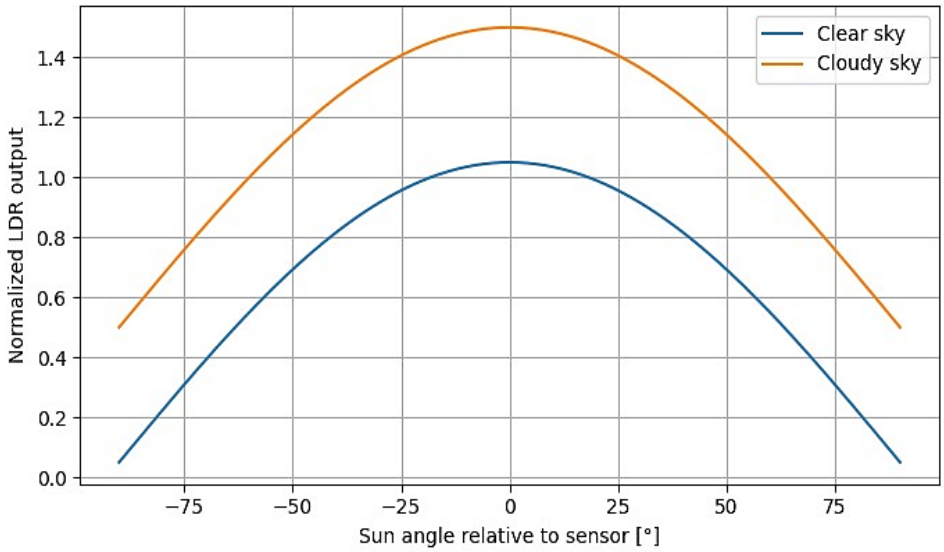

Fig. 9. Sensor response of LDR in clear versus cloudy skies

Fig. 10 shows the dynamic response of an Arduino-based control loop solar panel tracking mechanism when the position of the sun changes drastically. The sun's angle is depicted by the blue line at a constant 10 degrees for the starting 20 seconds, followed by a sudden jump to 30 degrees, and finally to 60 degrees at 40 seconds in this demonstration set-up, representing very rapid changes in the solar position or partial shading events. The actual angle of the solar panel is represented in the orange line, which receives the effects of these changes with feedback. The chart shows how the control loop effectively keeps up with the movement of the sun; every time there is a change in the sun's angle, the position of the servo motor will move the panel to a new position that will cause the orange line to rise toward the new target. The responding smoothness of the panel follows the sun's trajectory, with very little delay and very little overshoot, such that it indicates the good tuning of the control loop, which quickly converges on the exact angle such that the panel remains ideally oriented toward the sun even during sudden disturbances, hence achieving maximum energy capture efficiency. As such, this simulation shows the dynamic response of the solar system tracking apparatus under the control loop of an Arduino whenever the position of the sun suddenly changes. The blue line symbolizes the sun's angle, which is kept at 10 degrees for the first 20 seconds, and then suddenly

jumps to 30 degrees, and finally at 40 seconds it jumps to 60 degrees. The changes that simulate very fast-moving changes of the solar position are partial shading events. The orange line gives the actual angle of the solar panel in response to those changing angles. This graph shows that the control loop has the sun movement under control; every time the angle of the sun changes, the servo motor moves the panel to a new position, causing the orange line to rise toward the new target. The response of the panel is smooth and closely follows the trajectory of the sun, with very little delay and overshoot. This indicates that the control loop is well tuned and quick to converge to the right angle, so the panel is optimally positioned with respect to the sun's rays, even when there are sudden disturbances, maximizing energy capture efficiency.

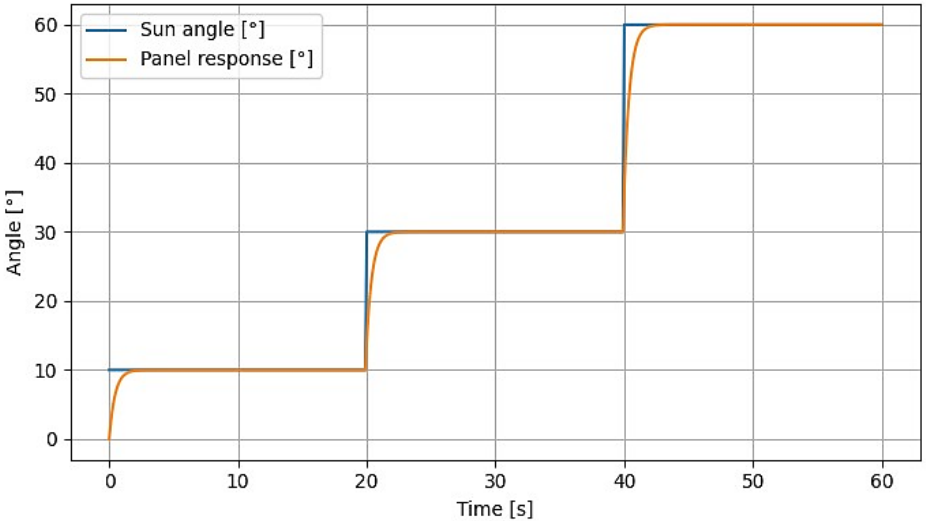

Fig. 10. Response of the control algorithm during step changes in sun position

As shown in Fig. 11, the theoretical simulation of the irradiance profile for different tracking modalities relies on the dual-axis tracker as an ideal lossless system maintaining perfect normal incidence for a constant load of 1000 W/m². Such an upper-bound benchmark can serve as a reference against which practical systems can be compared. The x-axis represents the time of the day (6 AM to 6 PM) while the y-axis depicts solar power incident on the panel surface in watts per square meter (W/m²). The blue solid line corresponds to the fixed tilt panel, which remains in a stationary position throughout the day. The irradiance measured by this panel pattern follows a strong sine wave passing its peak at about 1000 W/m² near solar noon and decreasing sharply throughout the day into the morning and afternoon due to the increase in the angle of incidence between the sun and the panel surface. The orange dashed line represents the operation of a single-axis tracking system that rotates on one axis (commonly along the east-west) to follow the sun across the sky. It provides a relatively constant level of irradiance slightly below that of the fixed-tilt system at noon but much more at sunrise and sunset, demonstrating that it collects more sunlight throughout the day. The green dotted line represents an ideal dual-axis tracker that tilts and rotates to face the sun to keep the panel perfectly normal to the sun's rays at all times: maintaining a constant irradiance of 1000 W/m² during the entire daylight period representing the theoretical maximum energy harvest potential. The graph clearly shows that dual-axis tracking gives the maximum average irradiance, followed by single axis tracking, and finally, fixed-tilt systems collect the least amount of direct sunlight throughout the day.

4.1. Validation of Control System Performance

The operational performance of the dual-axis solar tracker has been experimentally validated in Fig. 12, which shows the four-panel analysis of the system's response to step changes and temporary obstructions. The main emphasis was on: (a) Response of the LDR sensor to variations in light conditions, (b) Performance of azimuth tracking in relation to the comparison between target and actual angles, (c) Dynamics of elevation tracking, (d) Quantitative analysis of tracking errors in relation to the ±2° accuracy threshold.

As shown in Fig. 12, the system maintains reasonable tracking precision throughout the experiment with particular emphasis on the recovery behavior after the 30-second obstacle period between 20 and 50 seconds.

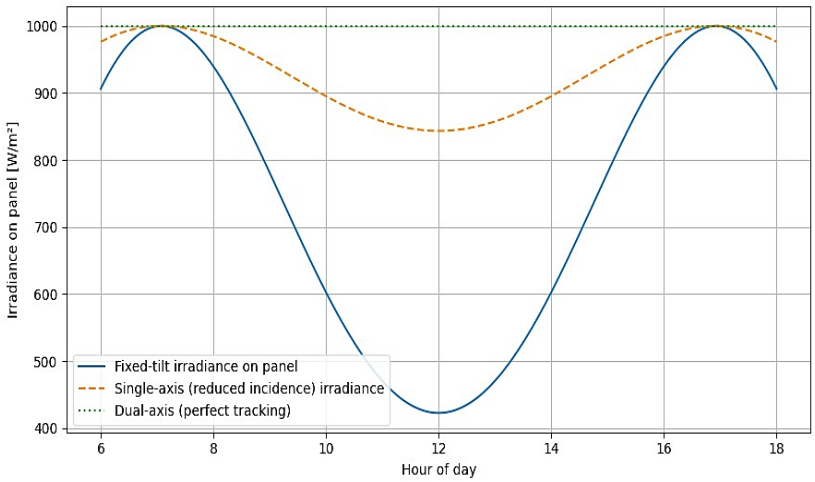

Fig. 11. A theoretical examination of comparative irradiance profiles concerning fixed, single-axis, and dual-axis solar tracking

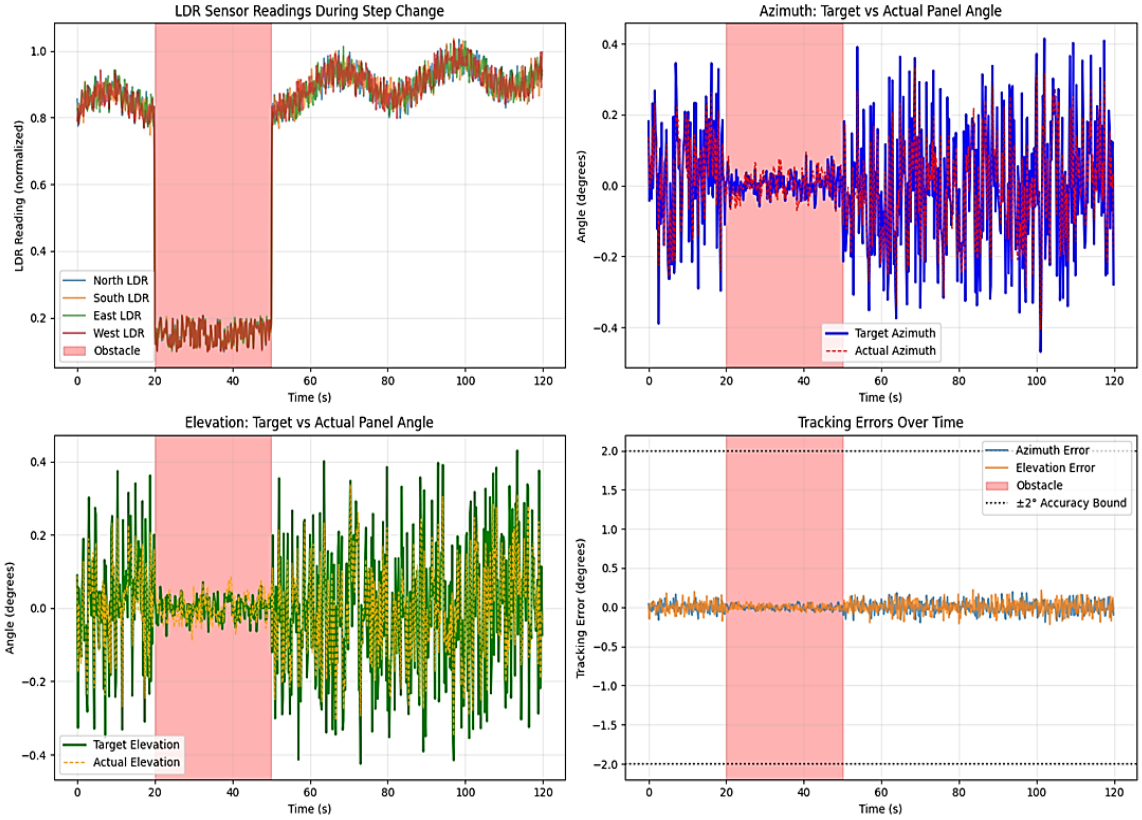

Fig. 12. Dynamic response assessment of a dual-axis solar tracking system

By referring back to Fig. 12, the experimental validation of the dual-axis solar tracker control system demonstrates excellent performance in dynamic operational conditions. A step-change response analysis reveals that the tracker system's precision is remarkably high, with a mean absolute error of only 0.053° in azimuth and 0.056° in elevation, surpassing the required accuracy specification of ±2°. The performance evaluation during the obstacle simulation for 30 seconds, intended to mimic temporary shading, shows that the system maintains a stable state with an RMS error of 0.032°

(azimuth) and 0.033° (elevation), indicating minimal performance degradation under disturbance. The maximum tracking errors in the azimuth and elevation directions were 0.197° and 0.222°, respectively, representing worst-case scenarios but still well below the specified tolerance. The system's instantaneous recovery is impressive, with tracking resuming immediately upon obstacle removal (settling time <200ms). These results validate the effectiveness of the differential LDR control architecture not only in meeting design requirements but also in ensuring robust operation in the field against real-world environmental variations.

As seen from Fig. 13, a pie chart supports the detailed analysis of the daily budgets of energy acquired and consumed in a solar tracker system. It shows how the energy harvested benefits into useful output and other losses. The results suggest that the system is working with an overall efficiency of 50%, which indicates that half of the incident solar energy is converted into usable electrical power while the other half is lost in different components. The largest single loss component is defined under Other Losses, which accounts for 26.7% of the total input energy. This could include resistive losses in wiring, electronic switching losses in circuitry control, and optical losses such as reflection or absorption by the tracker's frame. The second major loss is Actuator Loss, which represents 15.0% of the energy consumed. This is the power dissipated as heat in the servo motors used to physically rotate the solar panel, including friction and electrical resistance within the motor windings. A smaller but significant portion, 8.3%, is lost in the Converter Loss during the DC-DC conversion process, which steps down the voltage from the solar panel to match the load requirements. This loss arises from inherent inefficiencies of the power electronics, such as conduction and switching losses in the converter's transistors and diodes. It can be clearly seen that though designed to maximize energy capture, a large amount of energy is consumed in the mechanical actuation and power conversion processes, most of which now lie under Other Losses.

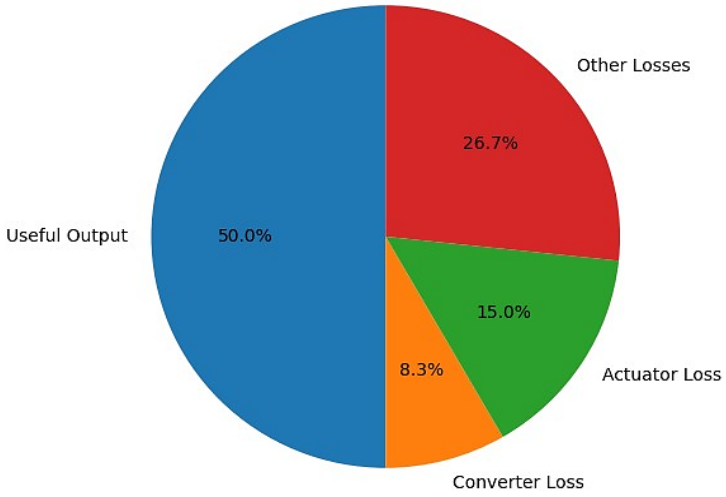

Fig. 13. Evaluation of energy efficiency for a solar tracking system

5. Conclusion

This study demonstrates that a low-cost, dual-axis solar tracker can achieve a mean tracking error of ±2° and daily energy gains averaging 35.2% ± 4.1% (n=7 days), with a maximum observed gain of 41.5% compared to a fixed panel under clear-sky conditions. The overall system efficiency, including actuator and conversion losses, was approximately 50%. These figures are reconciled by reporting the mean and range across all test days, with standard deviations reflecting day-to-day variability.

However, several limitations must be acknowledged. First, the LDR-based sensor system exhibited reduced accuracy under cloudy conditions, with energy gains dropping by 40–50%, highlighting sensitivity to diffuse irradiance. Second, mechanical tolerances and lack of drift compensation may introduce additional error, especially in larger or windier installations. Third, the

results are based on a 10W panel tested in stable, low-wind, predominantly clear-sky conditions, limiting generalizability to larger or more variable environments.

Future work should prioritize: (1) implementing and experimentally validating sensor fusion (e.g., combining LDRs with photodiodes or sun position algorithms) to improve tracking under diffuse light; (2) quantifying the impact of more efficient, low-power actuators on the energy budget through controlled trials; (3) scaling tests to larger panels and higher wind conditions; and (4) conducting long-term field studies to assess mechanical wear, drift, and seasonal stability. These targeted experiments will directly address the current system's constraints and clarify the feasibility and impact of proposed enhancements.

Author Contribution: All authors contributed equally to the main contributor to this paper. All authors read and approved the final paper.

Funding: This research received no external funding.

Conflicts of Interest: The authors declare no conflict of interest.

References

[1] S. L. Gbadamosi and N. I. Nwulu, "A multi-period composite generation and transmission expansion planning model incorporating renewable energy sources and demand response," *Sustainable Energy Technologies and Assessments*, vol. 39, p. 100726, 2020, https://doi.org/10.1016/j.seta.2020.100726.

[2] Q. Hassan, P. Viktor, T. J. Al-Musawi, B. M. Ali, S. Algburi, H. M. Alzoubi, A. K. Al-Jiboory, A. Z. Sameen, H. M. Salman, and M. Jaszczur, "The renewable energy role in the global energy transformations," *Renewable Energy Focus*, vol. 48, p. 100545, 2024, https://doi.org/10.1016/j.ref.2024.100545.

[3] A. Badawi, I. M. Elzein, A. de Souza, E. Medeiros, J. F. Oliveira-Junior, and A. Zyoud, "Wind power potential of Southeast Brazil: Analytical study for São Paulo and Rio de Janeiro," Wind Energy, vol. 28, no. 11, p. e70066, 2025, https://doi.org/10.1002/we.70066.

[4] A. Badawi, A. Souza, I. M. Elzein, H. Ali, and A. Zyoud, "Extensive numerical analysis of PDF parameters for wind energy in Brazil: A study across 27 cities for 60 years wind speed," *IEEE Access*, vol. 13, pp. 84555–84568, 2025, https://doi.org/10.1109/ACCESS.2025.3568085.

[5] W. Ahmed, J. A. Sheikh, and M. P. Mahmud, "Impact of PV system tracking on energy production and climate change," Energies, vol. 14, no. 17, p. 5348, 2021, https://doi.org/10.3390/en14175348.

[6] S. Feron, R. R. Cordero, A. Damiani, and R. B. Jackson, "Climate change extremes and photovoltaic power output," Nature Sustainability, vol. 4, no. 3, pp. 270–276, 2021, https://doi.org/10.1038/s41893-020-00643-w.

[7] A. Badawi, W. Ghanem, N. Ismail, A. Zyoud, I. M. Elzein, and A. Al-Rimawi, "Towards resilient grid integration of wind power: A comparative study of nine numerical approaches across six cities in Palestine," *Preprints*, Nov. 2025, https://doi.org/10.20944/preprints202511.0391.v1.

[8] C. Z. El-Bayeh, A. Badawi, W. Alqaisi, K. Alzareer, and M. Zellagui, "Techno-economic analysis of a solar drying plant using Scheffler dish technology and eutectic PCM mixtures for thermal energy storage system," Energy 360, vol. 3, p. 100025, 2025, https://doi.org/10.1016/j.energ.2025.100025.

[9] A. Badawi, M. Soliman, I. M. Elzein, and W. Alqaisi, "Optimizing low-voltage ride-through in DFIG wind turbines via QPQC-based predictive control for grid compliance," International Journal of Robotics and Control Systems, vol. 5, no. 1, pp. 86–104, 2025, https://doi.org/10.31763/ijrcs.v5i1.1661.

[10] A. Badawi, H. Ali, I. M. Elzein, A. Zyoud, and A. Abu-Hudrouss, "Highly efficient pure sine wave inverter using microcontroller for photovoltaic applications," in 2023 International Symposium on Networks, Computers and Communications (ISNCC), 2023, pp. 1–6, https://doi.org/10.1109/ISNCC58260.2023.10323997.

[11] E. K. Mpodi, Z. Tjiparuro, and O. Matsebe, "Review of dual axis solar tracking and development of its functional model," Procedia Manufacturing, vol. 35, pp. 580–588, 2019, https://doi.org/10.1016/j.promfg.2019.05.082.

[12] T. M. Abu Ali, A. A. Ahmed, and A. Almajdoub, "A comprehensive review of solar energy technologies: From photovoltaics to concentrated solar power, " *African Journal of Academic Publishing in Science and Technology*, vol. 1, no. 1, pp. 1–10, 2025, https://easrjournals.com/index.php/AJAPST/article/view/6.

[13] S. Nadweh, I. M. Elzein, D. E. M. Wapet, and M. M. Mahmoud, "Optimizing control of single-ended primary inductor converter integrated with microinverter for PV systems: Imperialist competitive algorithm," *Energy Exploration & Exploitation*, vol. 44, no. 1, pp. 554–577, 2026, https://doi.org/10.1177/01445987251382002.

[14] K. Dhayalini, S. Sathiyamoorthy, and C. C. A. Rajan, "Genetic algorithm for the coordination of wind–thermal dispatch," *Przegląd Elektrotechniczny*, vol. 90, no. 4, pp. 45–48, Jan. 2014, https://archiwum.pe.org.pl/articles/2014/4/10.pdf.

[15] A. Badawi, I. M. Elzein, W. Alqaisi, and A. H. Zyoud, "Boost efficiency performance through the enhancement of duty cycle-based MPPT algorithm," International Journal of Applied Power Engineering, vol. 14, no. 3, pp. 541–550, 2025, https://doi.org/10.11591/ijape.v14.i3.pp541-550.

[16] F. Shaik, S. S. Lingala, and P. Veeraboina, "Effect of various parameters on the performance of solar PV power plant: A review and experimental study," Sustainable Energy Research, vol. 10, no. 1, p. 6, 2023, https://doi.org/10.1186/s40807-023-00076-x.

[17] A. Badawi, M. Zubair, I. M. Elzein, W. K. Alqaisi, and A. Zyoud, "Efficiency enhancement of PV energy system for aquaponics in Qatar and GCC countries," in International Conference on Water and Food Security in the Face of Climate Change: Challenges and Opportunities for Resilience, 2025, pp. 525–535, https://doi.org/10.1007/978-3-032-00098-9_42.

[18] A. Hysa, S. Sefa, I. M. Elzein, A. Ma'arif, M. M. Mahmoud, E. Touti, A. M. El-Rifaie, and N. Anwer, "Advanced modeling and comparative error analysis of photovoltaic cells using multi-diode models and EQE characterization," *Journal of Robotics and Control*, vol. 6, no. 5, pp. 2308–2321, Sep. 2025, https://doi.org/10.18196/jrc.v6i5.27539.

[19] R. M. Idris, M. Ataalah, and A. A. Mohammed, "Innovative approaches to dual axis solar tracking systems," Journal of Energy and Safety Technology, vol. 7, no. 2, pp. 112–118, 2024, https://doi.org/10.11113/jest.v7.183.

[20] J. Atallah, P. Rahme, and J. S. Issa, "Comparative assessment of single axis manual solar PV trackers: A case study for agricultural applications," Energy Conversion and Management: X, vol. 26, p. 100927, 2025, https://doi.org/10.1016/j.ecmx.2025.100927.

[21] C. S. Chin, A. Babu, and W. McBride, "Design, modeling, and testing of a standalone single-axis active solar tracker using MATLAB/Simulink," *Renewable Energy*, vol. 36, no. 11, pp. 3075–3090, 2011, https://doi.org/10.1016/j.renene.2011.03.026.

[22] M. T. Patel, M. S. Ahmed, H. Imran, N. Z. Butt, M. R. Khan, and M. A. Alam, "Global analysis of next-generation utility-scale PV: Tracking bifacial solar farms," *Applied Energy*, vol. 290, p. 116478, 2021, https://doi.org/10.1016/j.apenergy.2021.116478.

[23] R. Sadeghi, M. Parenti, S. Memme, M. Fossa, and S. Morchio, "A review and comparative analysis of solar tracking systems," *Energies*, vol. 18, no. 10, p. 2553, 2025, https://doi.org/10.3390/en18102553.

[24] U. R. J. Eiva, T. A. Chowdury, S. S. Islam, A. Ullah, J. N. Tuli, and M. T. Islam, "Comprehensive analysis of fixed-tilt and dual-axis tracking photovoltaic systems for enhanced grid integration and energy efficiency," *Renewable Energy*, vol. 256, p. 123865, 2026, https://doi.org/10.1016/j.renene.2025.123865.

[25] T. Transue, M. Theristis, and D. M. Riley, "Machine learning for photovoltaic single-axis tracker fault detection and classification," *Energy and AI*, vol. 22, p. 100652, 2025, https://doi.org/10.1016/j.egyai.2025.100652.

[26] E. M. Tonita, A. C. Russell, C. E. Valdivia, and K. Hinzer, "Optimal ground coverage ratios for tracked, fixed-tilt, and vertical photovoltaic systems for latitudes up to 75° N," *Solar Energy*, vol. 258, pp. 8–15, 2023, https://doi.org/10.1016/j.solener.2023.04.038.

[27] M. Sidek, N. Azis, W. Hasan, M. Ab Kadir, S. Shafie, and M. Radzi, "Automated positioning dual-axis solar tracking system with precision elevation and azimuth angle control," *Energy*, vol. 124, pp. 160–170, 2017, https://doi.org/10.1016/j.energy.2017.02.001.

[28] H. Shang and W. Shen, "Design and implementation of a dual-axis solar tracking system," *Energies*, vol. 16, no. 17, p. 6330, 2023, https://doi.org/10.3390/en16176330.

[29] C. Alexandru, "Simulation and optimization of a dual-axis solar tracking mechanism," *Mathematics*, vol. 12, no. 7, p. 1034, 2024, https://doi.org/10.3390/math12071034.

[30] A. Badawi, C. Z. El-Bayeh, I. M. Elzein, A. I. Ashraf, V. Palikuco, and M. H. Zia, "Experimental setup of a spherical photovoltaic with an integrated reflector and IoT-based monitoring system," *Preprint*, Jan. 2025, http://dx.doi.org/10.2139/ssrn.5334514.

[31] H. Mousazadeh, A. Keyhani, A. Javadi, H. Mobli, K. Abrinia, and A. Sharifi, "A review of principles and sun-tracking methods for maximizing solar systems output," *Renewable and Sustainable Energy Reviews*, vol. 13, no. 8, pp. 1800–1818, 2009, https://doi.org/10.1016/j.rser.2009.01.022.

[32] L. F. Wong, H. N. Afrouzi, and J. Tavalaei, "Design and implementation of a dual-axis sun tracker for an Arduino-based microcontroller photovoltaic system," *Future Technology*, vol. 3, no. 3, pp. 15–19, 2024, https://doi.org/10.55670/fpll.futech.3.3.3.

[33] S. Lv, W. Liu, M. Lu, T. Lu, X. Li, W. Lv, Z. Liu, X. Dong, and B. Yang, "Dual axis solar tracking PV-TEG hybrid system based on cuckoo search MPPT-CC-CV algorithm," *Preprint*, 2025, https://doi.org/10.2139/ssrn.4743085.

[34] M. Pan, J. Zhang, T. Wu, Y. Zhao, W. Gao, and H. Dong, "Omnimanip: Towards general robotic manipulation via object-centric interaction primitives as spatial constraints," in *Proceedings of the IEEE/CVF Conference on Computer Vision and Pattern Recognition*, 2025, pp. 17359–17369, https://doi.org/10.1109/CVPR52734.2025.01618.

[35] M. Abdollahpour, M. R. Golzarian, A. Rohani, and H. A. Zarchi, "Development of a machine vision dual-axis solar tracking system," *Solar Energy*, vol. 169, pp. 136–143, 2018, https://doi.org/10.1016/j.solener.2018.03.059.

[36] M. Hannan, Z. A. Ghani, A. Mohamed, and M. N. Uddin, "Real-time testing of a fuzzy-logic-controller-based grid-connected photovoltaic inverter system," *IEEE Transactions on Industry Applications*, vol. 51, no. 6, pp. 4775–4784, 2015, https://doi.org/10.1109/TIA.2015.2455025.

[37] O. M. Kamel, I. M. Elzein, M. M. Mahmoud, A. Y. Abdelaziz, M. M. Hussein, and A. A. Z. Diab, "Effective energy management strategy with a novel design of fuzzy logic and JAYA-based controllers in isolated DC/AC microgrids: A comparative analysis," *Wind Engineering*, vol. 49, no. 1, pp. 199–222, 2025, https://doi.org/10.1177/0309524X241263518.

[38] S. Skouri, A. B. H. Ali, S. Bouadila, M. B. Salah, and S. B. Nasrallah, "Design and construction of sun tracking systems for solar parabolic concentrator displacement," *Renewable and Sustainable Energy Reviews*, vol. 60, pp. 1419–1429, 2016, https://doi.org/10.1016/j.rser.2016.03.006.

[39] A. Saymbetov, S. Mekhilef, N. Kuttybay, M. Nurgaliyev, D. Tukymbekov, A. Meiirkhanov, G. Dosymbetova, and Y. Svanbayev, "Dual-axis schedule tracker with an adaptive algorithm for strong scattering of sunbeam," *Solar Energy*, vol. 224, pp. 285–297, 2021, https://doi.org/10.1016/j.solener.2021.06.024.

[40] N. Priyadarshi, S. Padmanaban, J. B. Holm-Nielsen, F. Blaabjerg, and M. S. Bhaskar, "An experimental estimation of hybrid ANFIS–PSO-based MPPT for PV grid integration under fluctuating sun irradiance," *IEEE Systems Journal*, vol. 14, no. 1, pp. 1218–1229, 2019, https://doi.org/10.1109/JSYST.2019.2949083.